DNA-Dependent Protein Kinase Catalytic Subunit Prevents Ferroptosis in Retinal Pigment Epithelial Cells

Xueying Wang,[1] Xi Wang,[1] Zhenzhen Zhao,[1] Qian Wang,[1] Xiaoman Zhu,[1] Qingjian Ou,[1,2] Jing-Ying Xu,[1] Lixia Lu,[1] Furong Gao,[1] Juan Wang,[1] Yanlong Bi,[1] Guo-Tong Xu,[1] Caixia Jin,[1] and Haibin Tian[1,2]

[1]Department of Ophthalmology of Tongji Hospital and Laboratory of Clinical and Visual Sciences of Tongji Eye Institute, School of Medicine, Tongji University, Shanghai, China
[2]Department of Pharmacology, School of Medicine, Tongji University, Shanghai, China

Correspondence: Guo-Tong Xu, Department of Ophthalmology of Tongji Hospital and Laboratory of Clinical and Visual Sciences of Tongji Eye Institute, School of Medicine, Tongji University, 389 Xincun Rd., Shanghai 200065, China; gtxu@tongji.edu.cn.
Caixia Jin, Department of Ophthalmology of Tongji Hospital and Laboratory of Clinical and Visual Sciences of Tongji Eye Institute, School of Medicine, Tongji University, 389 Xincun Rd., Shanghai 200065, China; 12060@tongji.edu.cn.
Haibin Tian, Department of Ophthalmology of Tongji Hospital and Laboratory of Clinical and Visual Sciences of Tongji Eye Institute, School of Medicine, Tongji University, 389 Xincun Rd., Shanghai 200065, China; tianhb@tongji.edu.cn.

Xueying Wang and Xi Wang are co-first authors who contributed equally to this study.
GTX, CJ, and HT are co-corresponding authors who contributed equally to this study.

Received: October 28, 2024
Accepted: December 28, 2024
Published: January 22, 2025

Citation: Wang X, Wang X, Zhao Z, et al. DNA-dependent protein kinase catalytic subunit prevents ferroptosis in retinal pigment epithelial cells. *Invest Ophthalmol Vis Sci.* 2025;66(1):50. https://doi.org/10.1167/iovs.66.1.50

Purpose. The purpose of this study was to investigate the activated core kinases involved in the DNA damage responses (DDR) during ferroptosis of retinal pigment epithelial (RPE) cells in vitro and their regulatory effects on ferroptosis.

Methods. Ferroptosis was induced by erastin in induced RPE (iRPE) cells derived from human umbilical cord mesenchymal stem cells (hUCMSCs), hUCMSCs, and induced pluripotent stem cell-derived RPE (iPSC-RPE) cells. CCK8 was employed to measure the cell viability. Calcein/PI staining was used to detect the ferroptotic cells. The γ-H2AX, 8-oxoG, and phosphorylated DNA-dependent protein kinase catalytic subunit (DNA-PKcs) were determined through immunostaining. The phosphorylation of DNA-PKcs and ERK1/2 was determined by Western blotting. Lipid peroxides were detected by BODIPY581/591-C11 staining.

Results. The iRPE cells exhibited a stronger ability to resist ferroptosis compared to hUCMSCs. Ferroptosis induced DNA damage in cells, and DNA-PKcs was rapidly phosphorylated in iRPE cells on the treatment of erastin. In addition, inhibition of DNA-PKcs phosphorylation promoted ferroptosis in iRPE cells, suggesting that DNA-PKcs prevents ferroptosis. Meanwhile, DNA-PKcs inhibited ERK1/2 phosphorylation only at the early stage of ferroptosis induction, whereas ERK1/2 phosphorylation played a protective role in iRPE cells. Furthermore, erastin inducing DNA-PKcs phosphorylation and inhibition of its phosphorylation promoting ferroptosis were also verified in iPSC-RPE cells.

Conclusions. The present study elucidates that the key DDR kinase DNA-PKcs is activated and plays protective role during ferroptosis in RPE cells in vitro, which will provide new research targets and strategies for inhibiting ferroptosis in RPE cells.

Keywords: retinal pigment epithelial cells, ferroptosis, DNA damage response, DNA-PKcs

Iron ions are significantly elevated in the retinal pigment epithelial (RPE) cells of age-related macular degeneration (AMD) patients, especially in the macular region where iron deposition is increased,[1] and a typical AMD feature of large amounts of lipofuscin in the RPE is induced in patients with anemia treated with iron ions.[2] Vitreous cavity injection of iron ions in mice increases the level of iron ions in the RPE and neuroretina, resulting in damage.[3] Furthermore, in the sodium iodate–induced AMD model in mice, RPE cells show typical ferroptosis features,[4] and a variety of proteins and signaling pathways, such as HO-1 and FABP4, have been reported to be associated with ferroptosis in RPE cells.[5–7]

Ferroptosis is a process of cell death caused by the accumulation of lipid peroxides. It mainly includes two path-

ways to convert phosphatidylethanolamine into lipid peroxides, namely the nonenzymatic catalytic process promoted by the Fenton reaction and the catalytic process of iron-containing lipoxygenases.[8] It has been reported that lipid peroxides can cause DNA damage, such as base modification forming 8-oxodG,[9] and even cause strand breaks.[10] Lipid peroxides can also degrade to produce aldehydes, including malondialdehyde (MDA) and 4-hydroxynonenal (4-HNE). MDA can form 1,4-dihydropyridine adducts with primary amines,[11] and 4-HNE is able to cause DNA strand breaks.[12] RPE cells are prone to generating lipid peroxides because of their physiological functions. For instance, lipofuscin in RPE cells can induce lipid peroxidation reactions and reduce the efficacy of lysosomes and antioxidant enzyme systems.[13] The process of RPE cells phagocytizing the outer segment disc membranes (POS) requires a large amount of oxygen consumption. The peroxidases in the formed phagosomes can also generate a large amount of lipid peroxides by oxidizing the fatty acids in POS.[14] These results suggest that lipid peroxides produced in RPE cells have the potential to cause DNA damage.

DNA damage can promptly activate the DNA damage response (DDR) that detects and senses DNA damage, and activates the repair system to repair various forms of DNA damage. When DNA damage is not properly repaired, DDR will trigger the cell death program to eliminate the unrepaired cells. In mammalian cells, the core kinases of DDR include ataxia telangiectasia mutated protein (ATM), ATM Rad3-related protein (ATR), and DNA-dependent protein kinase catalytic subunit (DNA-PKcs).[15] These DDR kinases regulate the phosphorylation levels and activities of various effector proteins, including the genome integrity–related protein P53 that can regulate the process of ferroptosis.[16] In MDA-MB-231 breast cancer cells, inhibiting ATM is able to promote the nuclear translocation of MTF1 and the expression of FTH1, FT, and FPN1, regulate iron metabolism, and inhibit ferroptosis in MDA-MB-231 cells.[17] ATM regulates P53 to inhibit the expression of SLC7A11 and promotes ferroptosis in H1299 tumor cells.[18] In addition, P53 can also promote FDXR, ALOX15, and inhibit the expression of ACSL4 to promote ferroptosis.[19] Thus it is clear that DDR kinases and their downstream regulatory factors are involved in regulating ferroptosis. However, it is unclear whether DDR kinases are involved in and regulate ferroptosis in RPE cells.

We previously successfully transdifferentiated human umbilical cord mesenchymal stem cells (hUCMSCs) into induced RPE (iRPE) cells using key transcription factors.[20] Compared with the ARPE19 cell line, iRPE cells and induced pluripotent stem cell–derived RPE (iPSC-RPE) had more similar characteristics.[20] In this article, using iRPE cells as the in vitro RPE cell model, we will detect the activated DDR core kinases in iRPE cells undergoing ferroptosis and elaborate the relationship between DDR kinases and ferroptosis. In addition, the kinase function will be further verified in iPSC-RPE cells in vitro.

Material and Methods

Cell Culture

We differentiated iPSC into iPSC-RPE cells previously,[21] iPSC-RPE cells were cultured in DMEM/F12, 10% knockout serum replacement, 1% nonessential amino acids, 2 mM glutamine, 50 U/mL penicillin, and 50 mg/mL streptomycin (all from Invitrogen, Carlsbad, CA, USA), and 10 mM nicotinamide (Sigma, St. Louis, MO, USA) in dishes precoated with Matrigel (Corning, Charlotte, NC, USA). The iPSC-RPE cells at passage 8 were used in this study. The hUCMSCs at passage 2 were obtained from the Eastern Union Stem Cell and Gene Engineering Co., Ltd. (Tianjin, China) and cultured in DMEM/F12 containing 10% FBS at 37°C and 5% CO_2. The iRPE cells were cultured in DMEM/F12 containing 10% FBS at 37°C and 5% CO_2. The hUCMSCs and iRPE cells at passages 6–8 were used to compare their capacity to resistance to ferroptosis.

Cell Viability

Cell viability assay was performed following the protocol of the CCK-8 assay kit (Beyotime, Shanghai, China). In brief, cells were seeded in 96-well culture plates at a density of 1500 cells/well in DMEM/F12 containing 10% knockout serum replacement (for iPSC-RPE cells) or 10% FBS (for hUCMSCs and iRPE cells) and different dosages of erastin (0 to 50 µM; MedChemExpress, Shanghai, China), RSL3 (0 to 10 µM, MedChemExpress), ferric ammonium citrate (FAC, 0 to 10 mM, MedChemExpress), or ERK1/2 inhibitor U0126 (MedChemExpress), DNA-PKcs inhibitor KU-57788 (MedChemExpress). Twenty-four hours later, CCK-8 reagent was added to each well and incubated for two hours at 37°C. Using a microplate reader, the optical absorbance was measured at 450 nm.

Calcein AM/PI Staining

Cells were cultured in 96-well culture plate. For calcein AM/PI staining, cells were cultured in 100 µL of calcein AM/PI working solution (Beyotime) at 37°C for one hour. The samples were then examined by a fluorescence microscope (Olympus IX73; Olympus, Tokyo, Japan).

Immunostaining

For immunofluorescence analysis, cells and cryosections were permeabilized with 0.1% Triton X-100 (Sigma) for 10 minutes, washed with PBS, and then blocked with 3% BSA (Sigma) in PBS. The samples were incubated with the primary antibodies against 4-HNE, 8-oxoG (Abcam, Cambridge, UK), γ-H2AX (Proteintech, Rosemont, IL, USA), or p-DNA-PKcs (Abcam) overnight at 4°C. They were then washed three times with PBS, followed by incubation with the fluorescent secondary antibodies (Invitrogen) overnight at 4°C. A 4,6-diamidino-2-phenylindole dihydrochloride (Sigma) was used to indicate the nucleus. The samples were then examined by a fluorescence microscope (Olympus IX73; Olympus).

Western Blotting

The cells were lysed by RIPA buffer containing protease and phosphatase inhibitor (Sigma). The protein extracts (20 µg per sample) were separated by 10% SDS-PAGE gels and transferred onto polyvinylidene difluoride membranes (Millipore, Bedford, MA, USA). After being blocked with 5% BSA in TBST for one hour, membranes were incubated with primary antibodies against p-DNA-PKcs, DNA-PKcs, p-ATM, ATM, p-ATR, ATR (Abcam), p-ERK1/2, ERK1/2, and β-actin (Proteintech) for 12 hours at 4°C, followed by incubation with corresponding secondary antibodies for one hour at

Investigative Ophthalmology & Visual Science

room temperature. The blots were visualized with a chemiluminescence imaging system (Tanon 5200; Tanon Shanghai, China) and quantified with Image J software (Version 1.48v). To confirm that ATM and ATR could be phosphorylated, hUCMSCs were treated with 200 µM tert-Butyl hydroperoxide (TBHP; MK, Shanghai, China) for 24 hours, samples were subjected to Western blot.

Lipid Peroxide Analysis

Lipid Peroxide Analysis was performed according to previous report with modifications.[22] Cells were cultured in 96-well culture plate and treated with erastin or KU57788 for 12 hours, culture medium was changed with DMDM/F12 containing 5 µM BODIPY581/591-C11 (Invitrogen), and cells were further cultured for one hour. The samples were then examined by a fluorescence microscope (Olympus IX73). The production of lipid peroxides was quantified as the ratio of the cells with fluorescence of 510 wave length over the cells with fluorescence of 590 wave length.

Vitreous Injection of FAC

Six-week-old C57BL/6 female mice (Laboratory Animal Center of Tongji University, Shanghai, China) were used in this study. All the experimental mice had free access to water and standard rodent chow and were housed in a specific pathogen-free environment with a temperature of 25°C, a humidity of 40% to 70%, and a 12-hour light-dark cycle. All animal procedures were performed according to the institutional guidelines and the Guide for the Care and Use of Laboratory Animals issued by the NIH and the guidelines of the animal experimentation ethics committee of Tongji University (approved no. TJAA09623202), and in accordance with the Association for Research in Vision and Ophthalmology Statement for the use of Animals in Ophthalmic and Vision Research.

The experimental mice were anesthetized with 2% sodium pentobarbital. A channel was created by inserting a 30-gauge needle behind the limbus into the vitreous chamber, and 1 µL FAC (0.5 mM) was injected into the vitreous chamber. The control eyes received an injection of PBS. Mice were sacrificed with an overdose of sodium pentobarbital one day later, and eyes were collected and fixed for preparation of cryosections.

Statistical Analysis

All values are expressed as the mean ± SD. Data were analyzed using GraphPad Prism 9 software (GraphPad Software, San Diego, CA, USA). All statistical analyses were performed using Student's *t*-test, or one-way ANOVA and post hoc Bonferroni's test. Statistical significance was set at $P < 0.05$.

Results

The iRPE Cells Have a Stronger Ability to Resist Ferroptosis Compared to hUCMSCs

We previously transformed hUMCSCs into iRPE cells.[20] To compare the ability of these two types of cells to resist ferroptosis, different concentrations of erastin were used to induce ferroptosis in hUCMSCs and iRPE cells. A previous study[23] reported that 5 µM erastin is able to inhibit cystine-glutamate exchange and induces ferroptosis, and 10 µM erastin is able to induce ferroptosis in ARPE19 cells.[24] It was found that when the concentration of erastin reached 5 µM, the viability of hUCMSCs reduced markedly (Fig. 1A), and the viability of iRPE cells was also reduced, but it was significantly higher than that of hUCMSCs (Fig. 1A). With the increase of concentration, the viability of iRPE cells continuously decreased, and when the concentration of erastin was increased to 20 µM, iRPE cells underwent massive death, but the viability was still higher than that of hUCMSCs (Fig. 1A). We used PI to label the nuclei of the dead cells and further confirmed that iRPE cells have a stronger ability to resist ferroptosis compared to hUCMSCs (Figs. 1B, 1C). Staining with 4-HNE and BODIPY581/591-C11 demonstrated the reduced production of peroxidized lipids in iRPE cells compared to that in hUCMSCs (Figs. 1D–F). We used RSL3 or FAC to induce ferroptosis in cells and further proved that iRPE cells have a stronger ability to resist ferroptosis (Supplementary Fig. S1).

Ferroptosis Induces DNA Damage

The lipid peroxides produced by ferroptosis can cause DNA damage in cells.[9,10] We used erastin to induce ferroptosis in hUCMSCs and iRPE cells. Immunofluorescence staining revealed that 8-oxoG was positive in hUCMSCs after erastin treatment, whereas iRPE cells were weakly positive (Fig. 2A). We further found that the number of hUCMSCs with phosphorylated H2AX (γ-H2AX) was increased significantly, indicating that DNA damage occurred, although the number of γ-H2AX+ iRPE cells was significantly lower than that in hUCMSCs after erastin treatment (Figs. 2A, 2B), confirming that ferroptosis can induce DNA damage in hUCMSCs and iRPE cells, and iRPE cells have stronger resistance to erastin-induced DNA damage.

DNA-PKcs Inhibits Erastin-Induced Ferroptosis

DNA damage is able to promptly activate the DDR that detects and senses DNA damage, and activates the repair system to repair various forms of DNA damage.[15] Among them, ATM, ATR, and DNA-PKcs are upstream key regulatory proteins.[15] We detected the phosphorylation levels of ATM, ATR, and DNA-PKcs in hUCMSCs and iRPE cells (Figs. 3A, 3B). We found that under the stimulation of erastin, DNA-PKcs, rather than ATM and ATR, in iRPE cells was rapidly phosphorylated, and demonstrated a markedly higher level than that in hUCMSCs (Figs. 3A, 3B). We next treated cells with TBHP to induce apoptosis, and found that TBHP could trigger the phosphorylations of ATM and ATR (Supplementary Fig. S2), confirming that TBHP-induced apoptosis, rather than erastin-induced ferroptosis, can trigger the phosphorylations of ATM and ATR. To investigate if DNA-PKcs plays a protective role by preventing ferroptosis in iRPE cells, We used the inhibitor KU-57788 of DNA-PKcs to inhibit DNA-PKcs.[25] The results showed that when the concentration of KU-57788 reached 1 µM, it did not affect the cell viability, but when the concentration reached 10 µM, it could reduce the viability of iRPE cells (Fig. 3C), thus we used 1 µM KU-57788 to inhibit the phosphorylation of DNA-PKcs, it was able to markedly reduced phosphorylation of DNA-PKcs (Figs. 3D, 3E). When combined with erastin

Investigative Ophthalmology & Visual Science

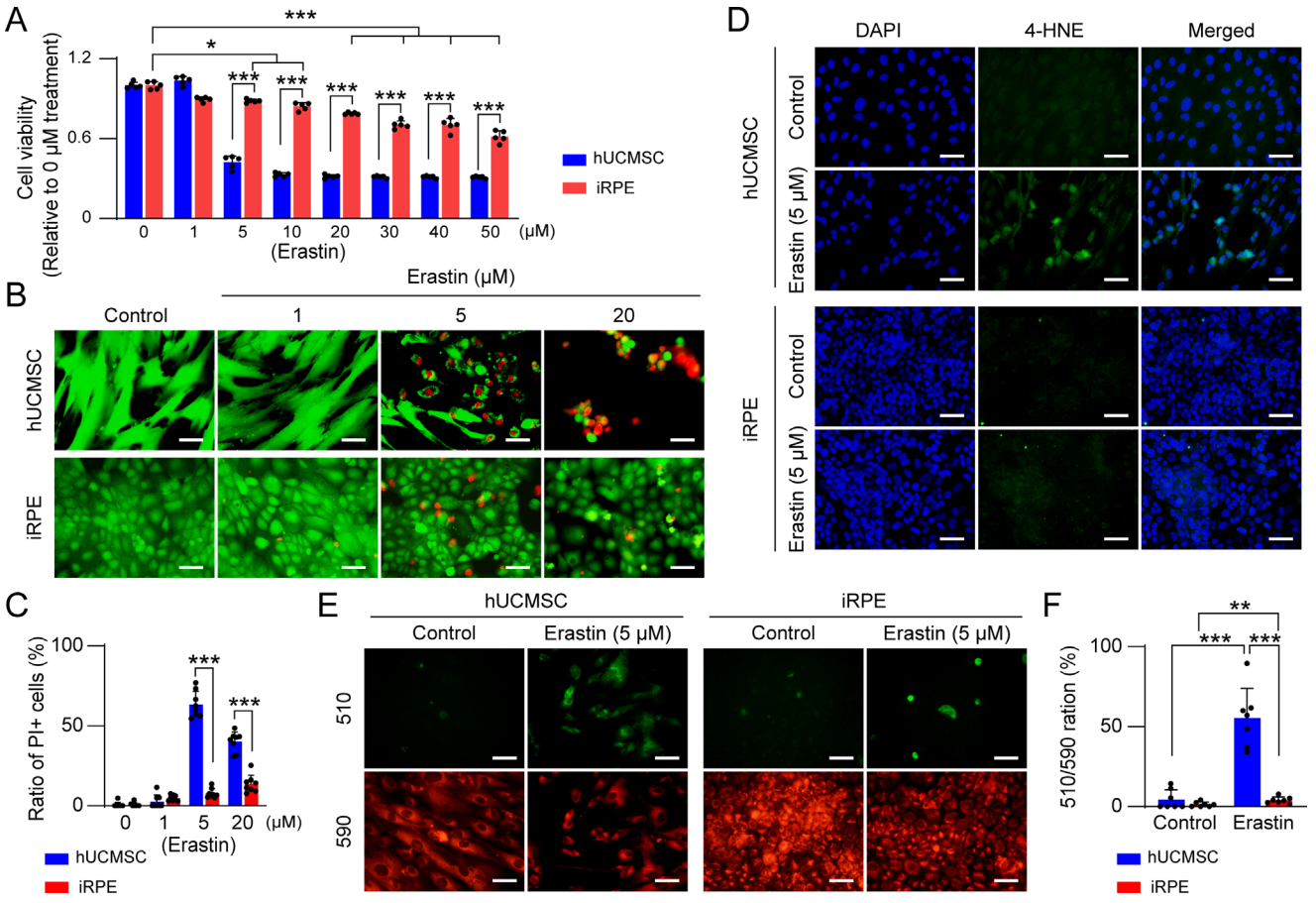

Figure 1. iRPE cells are more resistant to ferroptosis than hUCMSCs. (**A**) Ferroptosis was induced by erastin with different doses ($n = 5$ per dose), and cell viability was analyzed by the CCK-8 after cells were treated for 24 hours. (**B**) Calcein/PI staining revealed PI+ cells. *Scale bar:* 50 μm. (**C**) Quantitative analysis of the proportion of PI+ cells ($n = 8$). (**D**) 4-HNE immunostaining in representative micrographs of hUCMSCs and iRPE cells after treated with 5 μM erastin for 12 hours. *Scale bar:* 50 μm. (**E**) Peroxidized lipids were detected by BODIPY581/591-C11 staining after cells were treated with 5 μM erastin for 12 hours. (**F**) The production of peroxidized lipids was determined as the ratio of the cells with fluorescence of 510 wave length over the cells with fluorescence of 590 wave length ($n = 7$). Data are mean ± SD, $^{*}P < 0.05$, $^{**}P < 0.01$, $^{***}P < 0.001$ using Student's *t*-test or one-way ANOVA and post hoc Bonferroni's test.

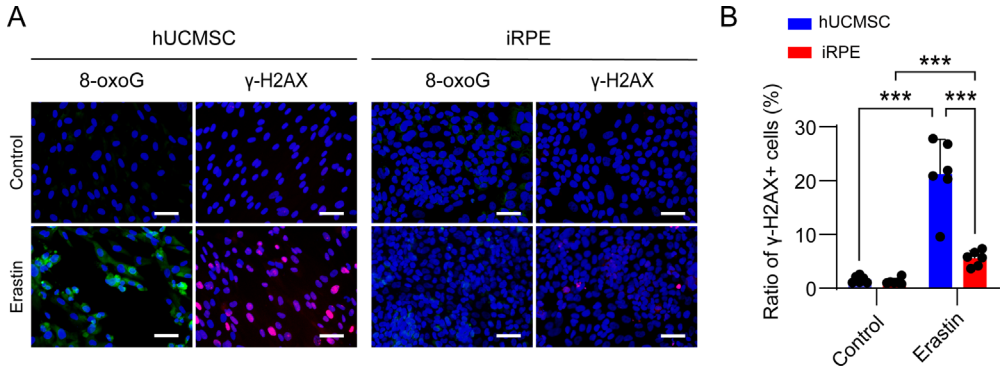

Figure 2. Ferroptosis induces DNA damages. (**A**) Immunostaining of 8-oxoG and γ-H2AX in hUCMSCs and iRPE was detected after treated with 5 μM erastin for 12 hours. *Scale bar:* 50 μm. (**B**) Quantitative analysis of γ-H2AX+ cells ($n = 6$). Data are mean ± SD, $^{***}P < 0.001$ using one-way ANOVA and post hoc Bonferroni's test.

to treat iRPE cells, inhibiting DNA-PKcs could increase the PI+ cells (Figs. 3F, 3G) and reduce the cell viability (Fig. 3H). We further analyzed the production of peroxidized lipids, and found that inhibiting the phosphorylation of DNA-PKcs by KU-57788 was able to increase the level of peroxidized lipids (Figs. 3I, 3J). These data suggest that DNA-PKcs play a protective role in iRPE cells by inhibiting ferroptosis.

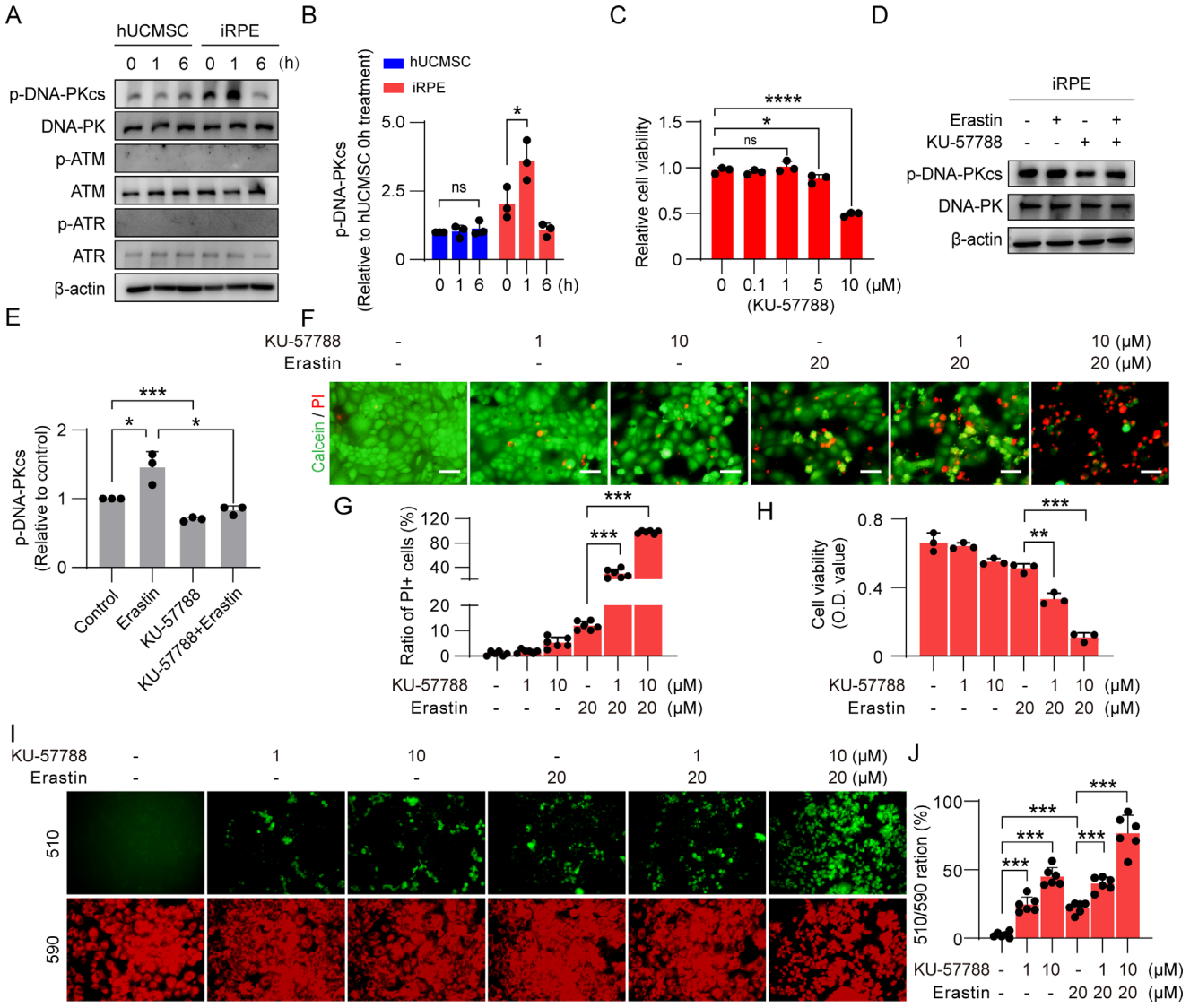

Figure 3. DNA-PKcs inhibits erastin-induced ferroptosis. (**A, B**) The phosphorylation of DNA-PKcs, ATM, and ATR was determined by (**A**) Western blot and (**B**) quantitative analysis of phosphorylation of DNA-PKcs after being treated with 20 μM erastin ($n = 3$) . (**C**) Cell viability was analyzed by the CCK-8 after iRPE cells were treated with KU-57788 for 24 hours ($n = 3$). (**D, E**) The phosphorylation of DNA-PKcs in iRPE cells was determined by (**D**) Western blot and (**E**) quantitative analysis ($n = 3$). (**F**) Calcein/PI staining revealed PI+ iRPE cells. *Scale bar:* 50 μm. (**G**) Quantitative analysis of the proportion of PI+ iRPE cells ($n = 6$). (**H**) Cell viability was analyzed by the CCK-8 after iRPE cells were treated with KU-57788 or erasin for 24 hours ($n = 3$). (**I**) Peroxidized lipids were detected by BODIPY581/591-C11 staining after cells were treated with KU-57788 or erastin for 12 hours. (**J**) The production of peroxidized lipids was determined as the ratio of the cells with fluorescence of 510 wave length over the cells with fluorescence of 590 wave length ($n = 6$). Data are mean ± SD, $^{*}P < 0.05$, $^{**}P < 0.01$, $^{***}P < 0.001$ using one-way ANOVA and post hoc Bonferroni's test.

DNA-PKcs has an Inhibitory Effect on Phosphorylation of ERK1/2

Previous studies have reported that erastin was able to promote the phosphorylation of ERK1/2, and phosphorylated ERK1/2 promoted ferroptosis.[26,27] We next investigated the phosphorylation of ERK1/2 in iRPE cells, and found that erastin can promote the phosphorylation of ERK1/2 in iRPE cells (Figs. 4A, 4B). However, in contrast to previous reports,[26,27] when we used U0126 to inhibit the phosphorylation of ERK1/2, we found that 2 μM U0126 significantly inhibited the phosphorylation of ERK1/2 and promoted ferroptosis in iRPE cells (Figs. 4A–E), proving that the phosphorylation of ERK1/2 plays a protective role in iRPE cells. U0126 2 μM alone did not change the viability of iRPE cells (Supplementary Fig. S3); thus we used 2 μM U0126 to inhibit the phosphorylation of ERK1/2 in this study. To demonstrate the relationship between DNA-PKcs and ERK1/2, we performed time course of phosphorylation of DNA-PKcs and ERK1/2 and showed that phosphorylation of ERK1/2 was later than that of DNA-PKcs, phosphorylated DNA-PKcs was detected one hour after erastin stimulation, and the phosphorylation level decreased after four hours, whereas the phosphorylation level of ERK1/2 was increased only after four hours (Figs. 4F–H). We further used the inhibitor of DNA-PKcs to inhibit DNA-PKcs and found that the phosphorylation level of ERK1/2 increased significantly (Figs. 4I, 4J), confirming that

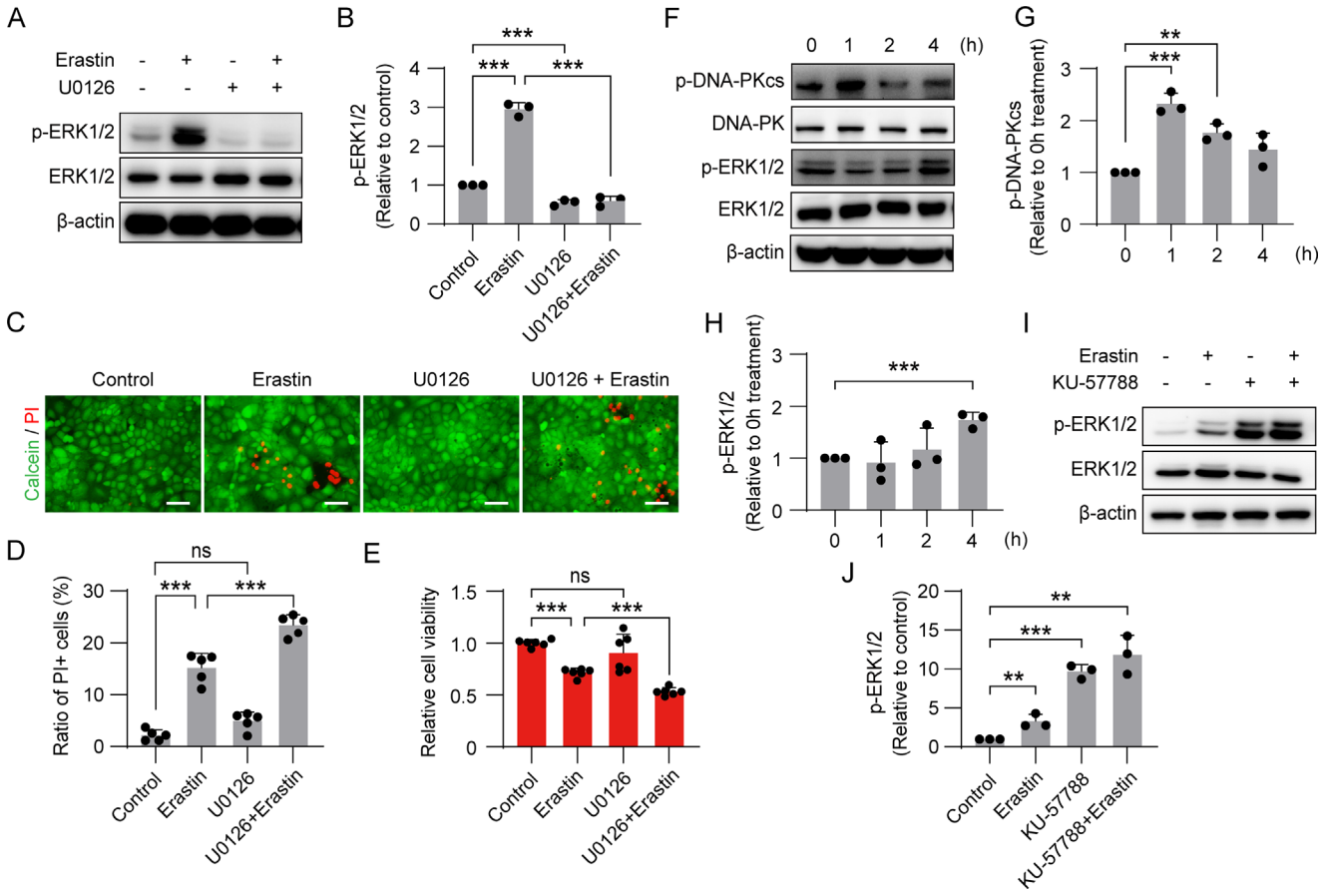

Figure 4. DNA-PKcs inhibits the phosphorylation of ERK1/2. (**A, B**) iRPE cells were treated with erastin or 2 µM U0126 for four hours, the phosphorylation of ERK1/2 was determined by (**A**) Western blot and (**B**) quantitative analysis ($n = 3$). (**C**) Calcein/PI staining revealed PI+ iRPE cells treated with 20 µM erastin or 2 µM U0126 for 12 hours. *Scale bar:* 50 µm. (**D**) Quantitative analysis of the proportion of PI+ iRPE cells ($n = 5$). (**E**) Cell viability was analyzed by the CCK-8 after iRPE cells were treated with erastin or U0126 for 24 hours ($n = 6$). (**F–H**) The time courses of phosphorylation of DNA-PKcs and ERK1/2 were determined by (**F**) Western blot and (**G, H**) quantitative analysis after treated with 20 µM erastin ($n = 3$). (**I, J**) The iRPE cells were treated with 20 µM erastin or 1 µM KU-57788 for four hours, and the phosphorylation of ERK1/2 was determined by (**I**) Western blot and (**J**) quantitative analysis ($n = 3$). Data are mean ± SD, $^{**}P < 0.01$, $^{***}P < 0.001$ using one-way ANOVA and post hoc Bonferroni's test.

DNA-PKcs exerts an inhibitory effect on the phosphorylation of ERK1/2, and the phosphorylation of ERK1/2 is increased after the phosphorylation level of DNA-PKcs is reduced.

DNA-PKcs Inhibits Ferroptosis in iPSC-RPE Cells

To further elaborate the role of DNA-PKcs in inhibiting ferroptosis in RPE cells, we obtained iPSC-RPE cells and verified the role of DNA-PKcs in inhibiting ferroptosis in iPSC-RPE cells. Using BODIPY581/591-C11 staining, we demonstrated that erastin induced iPSC-RPE cells to produce more lipid peroxides (Figs. 5A, 5B). In addition, erastin was also able to promote the phosphorylation of DNA-PKcs in iPSC-RPE cells (Figs. 5C, 5D), and the inhibitor KU-57788 of DNA-PKcs inhibited the phosphorylation of DNA-PKcs (Figs. 5C, 5D) and caused more iPSC-RPE cells to undergo ferroptosis (Figs. 5E, 5F). These results confirm that DNA-PKcs plays an inhibitory role in the process of ferroptosis in RPE cells. Iron ions are significantly elevated in the RPE cells of patients with AMD.[1] Intravitreal injection of iron ions can be used to simulate this process.[28] We injected iron ions into the eyes of mice and found that iron ions could activate the phosphorylation of DNA-PKcs in RPE cells (Supplementary Fig. S4), suggesting that DNA-PKcs can be used as a target for the treatment of AMD in the future.

Discussion

We determined that the DNA damage response was triggered during the ferroptosis process of RPE cells, and the core kinase DNA-PKcs was activated and was able to inhibit ferroptosis in RPE cells. Previous studies have reported that DNA-PKcs is a key protein kinase in nonhomologous end joining (NHEJ). DNA-PKcs and Ku70/80 bind DNA termini to assemble into the holoenzyme DNA-PK, which further recruits NHEJ-related ligases and repair proteins, including DNA ligase IV, XRCC4, XLF, and Artemis, promoting the occurrence of NHEJ.[29] ATM and ATR are involved in homologous recombination repair and are activated when DNA double-strand breaks occur.[30] However, we found that erastin could activate DNA-PKcs but did not activate ATM and ATR. Previous work reported that although inhibiting

Investigative Ophthalmology & Visual Science

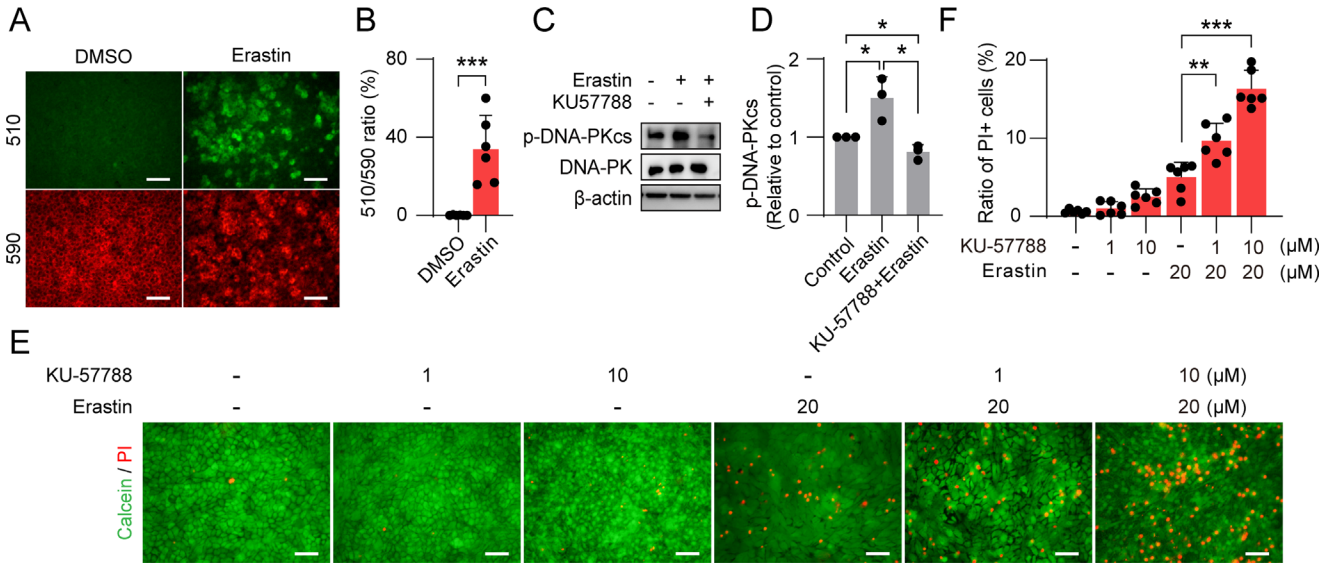

Figure 5. DNA-PKcs inhibits ferroptosis in iPSC-RPE cells. (**A, B**) Peroxidized lipids were detected by BODIPY581/591-C11 staining, the production of peroxidized lipids was determined as the ratio of the cells with fluorescence of 510 wave length over the cells with fluorescence of 590 wave length ($n = 6$). (**C, D**) iPSC-RPE cells were treated with erastin or KU-57788 for one hours, the phosphorylation of DNA-PKcs was determined by (**C**) Western blot and (**D**) quantitative analysis ($n = 3$). (**E**) Calcein/PI staining revealed PI+ iPSC-RPE cells treated with erastin or KU-57788 for 24 hours. *Scale bar:* 50 µm. (**F**) Quantitative analysis of the proportion of PI+ iRPE cells ($n = 6$). Data are mean ± SD, $^{*}P < 0.05$, $^{**}P < 0.01$, $^{***}P < 0.001$ using Student's *t*-test or one-way ANOVA and post hoc Bonferroni's test.

ATM can inhibit ferroptosis, the ferroptosis inducer erastin does not increase the phosphorylation level of ATM in MDA-MB-231 breast cancer cells.[17] These data demonstrated that DNA double-strand breaks may not occur during the ferroptosis process induced by erastin. Besides participating in DNA damage repair in the nucleus, DNA-PKcs has also been found in the cytoplasm,[31] lipid rafts,[32] cytoskeleton,[33] plasma membrane,[34] and mitochondria[35] and is involved in other biological reactions. For instance, DNA-PKcs interacts with glycolytic proteins ALDOA and PKM2 and phosphorylates them, promoting their activities.[36] DNA-PKcs interacts with the Wnt transcription factor LEF1 and is crucial for LEF1-mediated transcription. DNA-PKcs drives the progression of prostate cancer through transcriptional regulation of the Wnt signal.[37] Thus DNA-PKcs not only involved in DNA damage repair during RPE ferroptosis and is more likely to be directly involved in regulating ferroptosis. For example, DNA-PKcs may phosphorylate P53, and P53 can directly regulate the expression of ferroptosis-related proteins.[38] Furthermore, the use of KU-57788 to inhibit DNA-PKcs can promote the production of lipid peroxides, indicating that DNA-PKcs may directly participate in the process of inhibiting the production of lipid peroxides in RPE cells.

DNA damage induces phosphorylation of the serine residue at position 139 in the C-terminus of H2AX.[39] γ-H2AX is the initiating signal molecule of DNA damage, which can recruit a series of DDR proteins to the DNA damage sites and form a DDR functional complex, thereby activating and initiating DNA repair.[39] It is known that ATM, ATR, and DNA-PKcs can phosphorylate H2AX.[40] There are also reports that JNK and p38MAPK can phosphorylate H2AX.[41,42] We found that in hUCMSCs, ATM, ATR, and DNA-PKcs are not activated, indicating that the phosphorylation of H2AX may be activated by other kinases. The 8-oxoG is one of the biomarkers of DNA oxidative damage. When the intracellular oxidant level increases, such as lipid peroxides, they attack guanine in DNA and oxidize it to form 8-oxoG.[9] Therefore detecting the level of 8-oxoG in organisms can reflect the degree of oxidative stress in cells. The increased levels of γ-H2AX and 8-oxoG indicate that RPE cells do indeed suffer DNA damage during the process of ferroptosis.

Previous studies reported that the MAPK signaling pathway regulates and mediates the oxidative stress response of RPE cells induced by sodium iodate,[43] as well as oxidative stress-induced senescence.[44] Inhibiting the activation of ERK1/2 in RPE cells can inhibit the formation of geographic atrophy.[45] In laser-induced choroidal neovascularization, ERK1/2 in RPE cells can be activated, and inhibiting ERK1/2 can inhibit choroidal neovascularization.[46] All the studies focus on the apoptosis of RPE cells, but the role of ERK1/2 in ferroptosis of RPE cells is not clear. Previous studies reported that activation of MAPK signaling pathway promotes ferroptosis in other types of cells. Artesunate activates the p38 and ERK signaling pathway in glioblastoma cells, inducing ferroptosis in cells.[47] Chenodeoxycholic acid, a type of bile acid, decreases mitochondrial membrane potential and elevates mitochondrial calcium level, which results in the production of excessive reactive oxygen species. Elevated ROS further activates the p38 MAPK signaling pathway, which collaboratively promotes the accumulation of lipid droplets and promotes ferroptosis in AML cells.[48] MDA , the metabolite of lipid peroxide, can directly phosphorylate p38 MAP kinase.[49] Erastin can increase the expression of TfR1 by activating P38 and JNK, increase the intracellular iron ion concentration, and promote ferroptosis.[50] These results indicate that activation of MAPK signaling pathway promotes ferroptosis. However, a contrary report showed that activation of ERK1/2 could inhibit ferroptosis in neuronal cells induced by PM2.5 exposure.[51] In our study, inactivation of ERK1/2 promoted ferroptosis in RPE cells indicates that ERK1/2 may regulate specific signaling pathway in RPE cells.

Investigative Ophthalmology & Visual Science

It has been reported that using U0126 to inhibit ERK1/2 phosphorylation, or knockdown of ERK1 or ERK2 can significantly increase the phosphorylation of DNA-PKcs induced by etoposide.[52] Ectopic expression of constitutively active MEK1Q56P can reduce the phosphorylation of DNA-PKcs in etoposide-induced MCF7 cells.[52] These results indicate that ERK1/2 inhibits the activation of DNA-PKcs. However, we found that the phosphorylation of ERK1/2 in iRPE cells was later than that of DNA-PKcs, and DNA-PKcs had an inhibitory effect on the phosphorylation of ERK1/2 in the early stage. This might be due to ERK1/2 promoting cell proliferation, but after DNA damage, the proliferation of cells needs to be inhibited to give cells sufficient time to repair the damaged DNA. In addition, epithelial-mesenchymal transition (EMT) in RPE cells is an important event in AMD, especially in wet AMD. Oxidative stress can activate ERK1/2 to promote the EMT in RPE cells, and inhibiting the phosphorylation of ERK1/2 can suppress the occurrence of EMT in RPE cells.[53,54] Therefore DNA-PKcs inhibits the ERK1/2 signaling pathway, which not only inhibits ferroptosis in RPE cells but also may suppress the occurrence of EMT in RPE cells. The mechanism of DNA-PKcs inhibiting ERK1/2 phosphorylation needs more effort to clarify.

In summary, by comparing the ability of hUCMSCs and iRPE cells to resist ferroptosis and the expression differences of DDR kinases, we found that iRPE cells have a stronger ability to resist ferroptosis compared to the hUCMSCs. It was confirmed that DNA-PKcs was rapidly phosphorylated in iRPE cells under erastin stimulation, and inhibiting DNA-PKcs could promote ferroptosis in iRPE cells. In addition, DNA-PKcs only had an inhibitory effect on the phosphorylation of ERK1/2 in the early stage of ferroptosis induction, while the phosphorylation of ERK1/2 played a protective role in iRPE cells in the later stage. The protective role of DNA-PKcs was further verified in iPSC-RPE cells. This study clarified the activated key DDR kinase during the ferroptosis process of RPE cells and their role in regulating ferroptosis, which will provide new research targets and strategies for inhibiting ferroptosis in RPE cells.

Acknowledgments

Supported by grants from the Ministry of Science and Technology of China (2020YFA0113102), National Natural Science Foundation of China (81770942), and Natural Science Foundation of Shanghai (24ZR1470100).

Disclosure: **X. Wang**, None; **X. Wang**, None; **Z. Zhao**, None; **Q. Wang**, None; **X. Zhu**, None; **Q. Ou**, None; **J.-Y. Xu**, None; **L. Lu**, None; **F. Gao**, None; **J. Wang**, None; **Y. Bi**, None; **G.-T. Xu**, None; **C. Jin**, None; **H. Tian** None

References

1. Biesemeier A, Yoeruek E, Eibl O, Schraermeyer U. Iron accumulation in Bruch's membrane and melanosomes of donor eyes with age-related macular degeneration. *Exp Eye Res*. 2015;137:39–49.
2. Song D, Kanu LN, Li Y, et al. AMD-like retinopathy associated with intravenous iron. *Exp Eye Res*. 2016;151:122.
3. Shu W, Baumann BH, Song Y, Liu Y, Wu X, Dunaief JL. Ferrous but not ferric iron sulfate kills photoreceptors and induces photoreceptor-dependent RPE autofluorescence. *Redox Biol*. 2020;34:101469.
4. Tang Z, Ju Y, Dai X, et al. HO-1-mediated ferroptosis as a target for protection against retinal pigment epithelium degeneration. *Redox Biol*. 2021;43:101971.
5. Chao C, Yang K, He D, Yang B. Induction of ferroptosis by HO-1 contributes to retinal degeneration in mice with defective clearance of all-trans-retinal. *Free Radic Biol Med*. 2023;194:245–254.
6. Liu Y, Wu D, Fu Q, et al. CHAC1 as a novel contributor of ferroptosis in retinal pigment epithelial cells with oxidative damage. *Int J Mol Sci*. 2023;24:1582.
7. Fan X, Xu M, Ren Q, et al. Downregulation of fatty acid binding protein 4 alleviates lipid peroxidation and oxidative stress in diabetic retinopathy by regulating peroxisome proliferator-activated receptor γ-mediated ferroptosis. *Bioengineered*. 2022;13:10540.
8. Stoyanovsky DA, Tyurina YY, Shrivastava I, et al. Iron catalysis of lipid peroxidation in ferroptosis: regulated enzymatic or random free radical reaction? *Free Radic Biol Med*. 2018;133:153.
9. Park J-W, Floyd RA. Lipid peroxidation products mediate the formation of 8-hydroxydeoxyguanosine in DNA. *Free Radic Biol Med*. 1992;12:245–250.
10. Inouye S. Site-specific cleavage of double-strand DNA by hydroperoxide of linoleic acid. *FEBS Lett*. 1984;172:231–234.
11. Esterbauer H, Schaur RJ, Zollner H. Chemistry and biochemistry of 4-hydroxynonenal, malonaldehyde and related aldehydes. *Free Radic Biol Med*. 1991;11:81–128.
12. Ji Y, He Y, Yang Y, Dai Z, Wu Z. Hydroxyproline alleviates 4-hydroxy-2-nonenal-induced DNA damage and apoptosis in porcine intestinal epithelial cells. *Anim Nutr*. 2022;9:7–15.
13. Shamsi FA, Boulton M. Inhibition of RPE lysosomal and antioxidant activity by the age pigment lipofuscin. *Invest Ophthalmol Vis Sci*. 2001;42:3041–6.
14. Zhang Z-Y, Bao X-L, Cong Y-Y, Fan B, Li G-Y. Autophagy in age-related macular degeneration: a regulatory mechanism of oxidative stress. *Oxid Med Cell Longev*. 2020;2020:2896036.
15. Qian J, Liao G, Chen M, et al. Advancing cancer therapy: new frontiers in targeting DNA damage response. *Front Pharmacol*. 2024;15:1474337.
16. Chen P-H, Tseng WH-S, Chi J-T. The intersection of DNA damage response and ferroptosis—a rationale for combination therapeutics. *Biology*. 2020;9:187.
17. Chen P-H, Wu J, Ding CK, et al. Kinome screen of ferroptosis reveals a novel role of ATM in regulating iron metabolism. *Cell Death Differ*. 2019;27:1008.
18. Jiang L, Kon N, Li T, et al. Ferroptosis as a p53-mediated activity during tumour suppression. *Nature*. 2015;520:57.
19. Xu R, Wang W, Zhang W. Ferroptosis and the bidirectional regulatory factor p53. *Cell Death Discov*. 2023;9:197.
20. Zhu X, Chen Z, Wang L, et al. Direct conversion of human umbilical cord mesenchymal stem cells into retinal pigment epithelial cells for treatment of retinal degeneration. *Cell Death Dis*. 2022;13:785.
21. Tian H, Chen Z, Zhu X, et al. Induced retinal pigment epithelial cells with anti-epithelial-to-mesenchymal transition ability delay retinal degeneration. *iScience*. 2022;25:105050.
22. Lee J-J, Chang-Chien GP, Lin S, et al. 5-Lipoxygenase inhibition protects retinal pigment epithelium from sodium iodate-induced ferroptosis and prevents retinal degeneration. *Oxid Med Cell Longev*. 2022;2022:1792894.
23. Dixon SJ, Patel DN, Welsch M, et al. Pharmacological inhibition of cystine–glutamate exchange induces endoplasmic reticulum stress and ferroptosis. *eLife*. 2014;3:e02523.
24. Sun Y, Zheng Y, Wang C, Liu Y. Glutathione depletion induces ferroptosis, autophagy, and premature cell senes-

cence in retinal pigment epithelial cells. *Cell Death Dis*. 2018;9:753.
25. Zhang J, Jing L, Tan S, et al. Inhibition of miR-1193 leads to synthetic lethality in glioblastoma multiforme cells deficient of DNA-PKcs. *Cell Death Dis*. 2020;11:602.
26. Savic D, Steinbichler TB, Ingruber J, et al. Erk1/2-dependent HNSCC cell susceptibility to erastin-induced ferroptosis. *Cells*. 2023;12:336.
27. Zalyte E, Cicenas J. Starvation mediates pancreatic cancer cell sensitivity to ferroptosis via ERK1/2, JNK and changes in the cell mesenchymal state. *Int J Mol Med*. 2022; 49:84.
28. Liu Y, Bell BA, Song Y, et al. Intraocular iron injection induces oxidative stress followed by elements of geographic atrophy and sympathetic ophthalmia. *Aging Cell*. 2021;20:e13490.
29. Yue X, Bai C, Xie D, Ma T, Zhou P-K. DNA-PKcs: a multifaceted player in DNA damage response. *Front Genet*. 2020;11:607428.
30. Chen P-H, Tseng WH-S, Chi J-T. The intersection of DNA damage response and ferroptosis—a rationale for combination therapeutics. *Biology*. 2020;9:187.
31. Ferguson BJ, Mansur DS, Peters NE, Ren H, Smith GL. DNA-PK is a DNA sensor for IRF-3-dependent innate immunity. *Elife*. 2012;1:e00047.
32. Lucero H, Gae D, Taccioli GE. Novel localization of the DNA-PK complex in lipid rafts: a putative role in the signal transduction pathway of the ionizing radiation response. *J Biol Chem*. 2003;278:22136–22143.
33. Kotula E, Faigle W, Berthault N, et al. DNA-PK target identification reveals novel links between DNA repair signaling and cytoskeletal regulation. *Plos One*. 2013;8: e80313.
34. Feng J, Park J, Cron P, Hess D, Hemmings BA. Identification of a PKB/Akt hydrophobic Motif Ser-473 kinase as DNA-dependent protein kinase. *J Biol Chem*. 2004;279:41189–41196.
35. Chen W-M, Chiang JC, Shang Z, et al. DNA-PKcs and ATM modulate mitochondrial ADP-ATP exchange as an oxidative stress checkpoint mechanism. *EMBO J*. 2023;42:e112094.
36. Dylgjeri E, Kothari V, Shafi AA, et al. A novel role for DNA-PK in metabolism by regulating glycolysis in castration-resistant prostate cancer. *Clin Cancer Res*. 2022;28: 1446.
37. Kothari V, Goodwin JF, Zhao SG, et al. DNA-dependent protein kinase drives prostate cancer progression through transcriptional regulation of the Wnt signaling pathway. *Clin Cancer Res*. 2019;25:5608.
38. Xu R, Wang W, Zhang W. Ferroptosis and the bidirectional regulatory factor p53. *Cell Death Discov*. 2023;9:197.
39. Owiti NA, Nagel ZD, Engelward BP. Fluorescence sheds light on DNA damage, DNA repair, and mutations. *Trends Cancer*. 2021;7:240–248.
40. Ban ´ath JP, MacPhail SH, Olive PL. Radiation sensitivity, H2AX phosphorylation, and kinetics of repair of DNA strand breaks in irradiated cervical cancer cell lines. *Cancer Res*. 2004;64:7144.
41. Lu C, Shi Y, Wang Z, et al. Serum starvation induces H2AX phosphorylation to regulate apoptosis via p38 MAPK pathway. *FEBS Lett*. 2008;582:2703–2708.
42. Lu C, Shi Y, Wang Z, et al. Cell apoptosis: requirement of H2AX in DNA ladder formation, but not for the activation of caspase-3. *Mol Cell*. 2006;23:121–132.
43. Tsou S-C, Chuang CJ, Hsu CL, et al. The novel application of EUK-134 in retinal degeneration: preventing mitochondrial oxidative stress-triggered retinal pigment epithelial cell apoptosis by suppressing MAPK/p53 signaling pathway. *Environ Toxicol*. 2025;40:88–100.
44. Zhu D, Wu J, Spee C, Ryan SJ, Hinton DR. BMP4 mediates oxidative stress-induced retinal pigment epithelial cell senescence and is overexpressed in age-related macular degeneration. *J Biol Chem*. 2009;284:9529–9539.
45. Dridi S, Hirano Y, Tarallo V, et al. ERK1/2 activation is a therapeutic target in age-related macular degeneration. *Proc Natl Acad Sci USA*. 2012;109:13781–13786.
46. Bin Y, Liu Y, Jiang S, Peng H. Elevated YKL-40 serum levels may contribute to wet age-related macular degeneration via the ERK1/2 pathway. *FEBS Open Bio*. 2021;11:2933–2942.
47. Song Q, Peng S, Che F, Zhu X. Artesunate induces ferroptosis via modulation of p38 and ERK signaling pathway in glioblastoma cells. *J Pharmacol Sci*. 2022;148:300–306.
48. Liu J. Chenodeoxycholic acid suppresses AML progression through promoting lipid peroxidation via ROS/p38 MAPK/DGAT1 pathway and inhibiting M2 macrophage polarization. *Redox Biol*. 2022;56:102452.
49. Folden DV, Gupta A, Sharma AC, Li SY, Saari JT, Ren J. Malondialdehyde inhibits cardiac contractile function in ventricular myocytes *via* a p38 mitogen-activated protein kinase-dependent mechanism. *Br J Pharmacol*. 2003;139:1310–1316.
50. Ye F, Chai W, Xie M, et al. HMGB1 regulates erastin-induced ferroptosis via RAS-JNK/p38 signaling in HL-60/NRASQ61L cells. *Am J Cancer Res*. 2019;9:730.
51. Xiong Q, Tian X, Xu C, et al. PM.5 exposure-induced ferroptosis in neuronal cells via inhibiting ERK/CREB pathway. *Environ Toxicol*. 2022;37:2201–2213.
52. Wei F, Yan J, Tang D, et al. Inhibition of ERK activation enhances the repair of double-stranded breaks via non-homologous end joining by increasing DNA-PKcs activation. *Biochim Biophys Acta*. 2013;1833:90–100.
53. Yang Y-C, Chien Y, Yarmishyn AA, et al. Inhibition of oxidative stress-induced epithelial-mesenchymal transition in retinal pigment epithelial cells of age-related macular degeneration model by suppressing ERK activation. *J Adv Res*. 2023;60:141–157.
54. Kim S-J, Kim YS, Kim JH, et al. Activation of ERK1/2-mTORC1-NOX4 mediates TGF-β1-induced epithelial-mesenchymal transition and fibrosis in retinal pigment epithelial cells. *Biochem Biophys Res Commun*. 2020;529: 747–752.

Investigative Ophthalmology & Visual Science